

Single Impurity In Ultracold Fermi Superfluids

Lei Jiang¹, Leslie O. Baksmaty¹, Hui Hu², Yan Chen³ and Han Pu¹

¹*Department of Physics and Astronomy, and Rice Quantum Institute, Rice University, Houston, TX 77251, USA*

²*ARC Centre of Excellence for Quantum-Atom Optics,
Centre for Atom Optics and Ultrafast Spectroscopy,*

Swinburne University of Technology, Melbourne 3122, Australia

³*Laboratory of Advanced Materials and Department of Physics, Fudan University, Shanghai 200433, China*

(Dated: June 1, 2019)

Impurities can be used as probes to detect material properties and to understand quantum phenomena. Here we study the effect of a single classical impurity in ultracold s -wave Fermi superfluids. The impurity can be either magnetic or non-magnetic. Although a non-magnetic impurity does not change macroscopic properties of the system, a magnetic impurity can induce a mid-gap bound state located inside the pairing gap. In addition, magnetic impurity can locally induce population imbalance in the system, potentially providing a method to realize FFLO-like state in a controlled way. We also propose a modified RF spectroscopy to measure the local density of states, as a cold-atom analog of STM.

PACS numbers: 03.75.Ss, 05.30.Fk, 71.10.Pm, 03.75.Hh

Ultracold atoms represent a many-body quantum system amenable to exquisite experimental control, which provides great advantages compared with conventional quantum many-body systems realized using, e.g., solid state materials. In condensed matter experiments, one big problem is the unavoidable defects contained in the material. This motivates the study of impurities in many-body systems, which turns out to be one of the great treasures in condensed matter physics. Impurities, for example, can be used as probes to detect material properties [1, 2]. In solid state, single impurity has been used to detect pairing symmetries in unconventional superconductors [3]. Impurities can also be used to demonstrate quantum mechanical principles such as the Friedel oscillation [4]. In strongly correlated systems, impurities can be used to pin one of the competing orders [5]. The cold atom system is intrinsically clean. However, disorder can be introduced on purpose, by employing, for example, laser speckles or quasiperiodic lattices [6]. Controllable manipulation of individual impurities in cold atom systems can also be realized using off-resonant laser light or another species of atoms/ions [7]. Such impurities can be either localized as point defects or extended; either static or dynamic. Their characters can be tuned accurately, which provides an exciting possibility to probe and to manipulate the properties of cold atoms.

In this Letter, we demonstrate this possibility by focusing on a single classical static impurity in an s -wave Fermi superfluid, to be treated as a potential scattering without internal degrees of freedom. Two different kinds of classical impurities are studied: One is non-magnetic, which scatters each spin species equally. The other is magnetic which scatters each spin species differently. We show that the impurity induces some intriguing bound states, which are known theoretically in solid state physics but have never been explored experimentally in-depth. We propose that these bound states can be probed using a modified radio-frequency (RF) spectroscopy technique

that is the analog of the widely used scanning tunneling microscope (STM) in solid state. We show also that the impurity in cold atoms may have wider applications than in conventional solid state systems: It is possible to generate novel exotic quantum states such as inhomogeneous superfluids.

We start by considering a one-dimensional system at zero temperature, although the calculation can be extended to higher dimensions straightforwardly. The Hamiltonian of the system can be written as,

$$H = \sum_{\sigma=\uparrow,\downarrow} \int dx \psi_{\sigma}^{\dagger} \left[-\frac{\hbar^2}{2m} \frac{d^2}{dx^2} - \mu_{\sigma} + V_T \right] \psi_{\sigma} + g \int dx \psi_{\uparrow}^{\dagger} \psi_{\downarrow}^{\dagger} \psi_{\downarrow} \psi_{\uparrow} + \sum_{\sigma=\uparrow,\downarrow} \int dx \psi_{\sigma}^{\dagger} U_{\sigma} \psi_{\sigma}, \quad (1)$$

where $\psi_{\sigma}^{\dagger}(x)$ and $\psi_{\sigma}(x)$ are, respectively, the fermionic creation and annihilation operators for spin species σ . $V_T(x)$ is the trapping potential which is usually taken to be harmonic. g is the strength of the interatomic interaction. In this work, we let g to be small and negative so that the system is a Bardeen-Cooper-Schrieffer (BCS) superfluid at low temperatures. The last term of the Hamiltonian describes the effect of the impurity which is represented by a scattering potential, $U_{\sigma}(x)$. For non-magnetic impurity, we have $U_{\uparrow}(x) = U_{\downarrow}(x)$; while for magnetic impurity, $U_{\uparrow}(x) = -U_{\downarrow}(x)$. Note that a general impurity potential can be decomposed into a sum of a magnetic part and a non-magnetic part. The impurity can be either a localized potential which can be approximated by a δ -function form $U_{\sigma}(x) = u_{\sigma} \delta(x)$, or can be an extended potential which we take to be a Gaussian with finite width. In the following, we will consider these two cases separately.

Localized impurity — Let us first consider a localized impurity with $U_{\sigma}(x) = u_{\sigma} \delta(x)$. If we are only interested in the effect of the impurity near its vicinity, we may neglect the trapping potential. Such a system can be then

conveniently studied using the T -matrix formalism [8]. As a result of the δ -function impurity potential, the T -matrix is momentum independent and analytical results can be obtained. The full Green's function G is related to the bare (i.e., in the absence of the impurity) Green's function G_0 and the T -matrix in the following way,

$$G(k, k', \omega) = G_0(k, \omega)\delta_{kk'} + G_0(k, \omega)T(\omega)G_0(k', \omega), \quad (2)$$

where ω is the frequency, k and k' represent the incoming and outgoing momenta in the scattering event, respectively. In the superfluid state, we introduce Nambu operator $\Psi_k^\dagger = (c_{k\uparrow}^\dagger, c_{-k\downarrow})$, so that $G = -\langle T_\tau \Psi_k(\tau) \Psi_{k'}^\dagger(0) \rangle$, G_0 and T are 2×2 matrices in particle-hole Nambu space. For the s -wave BCS superfluid, the bare Green's function is given by

$$G_0(k, \omega) = \frac{\omega\sigma_0 + (\epsilon_k - \tilde{\mu})\sigma_3 - \Delta\sigma_1}{\omega^2 - (\epsilon_k - \tilde{\mu})^2 - \Delta^2}, \quad (3)$$

where $\epsilon_k = \hbar^2 k^2 / (2m)$, σ_i are the Pauli matrices (σ_0 is the identity matrix) and Δ the s -wave pairing gap. Here the effective chemical potential, $\tilde{\mu} = \mu - gn(x)$, includes the contribution from the Hartree term, where $n(x)$ is the local density for one spin species. For non-magnetic impurity, we take $u = u_\uparrow = u_\downarrow$, the T -matrix is given by

$$T^{-1}(\omega) = u^{-1}\sigma_3 - \sum_k G_0(k, \omega), \quad (4)$$

while for magnetic impurity, we take $u = u_\uparrow = -u_\downarrow$, and the corresponding T -matrix has the same form as in Eq. 4 with σ_3 replaced by σ_0 . From the full Green's function, one can immediately obtain the local density of states (LDOS) at the impurity site as

$$\rho(\epsilon) = -\frac{1}{\pi} \sum_{k, k'} \text{Im} [G(k, k', \epsilon + i0^+)]. \quad (5)$$

The solid line in Fig. 1 shows the LDOS at impurity site obtained from the T -matrix method for an attractive non-magnetic impurity with $u < 0$. The important features one can easily notice are the superfluid gap near $\epsilon = 0$ (the energy is measured relative to the Fermi energy), and a strong peak below the Fermi sea which represents the bound state induced by the impurity potential. The bound state energy can be obtained analytically as $E_0 = -\sqrt{[\tilde{\mu} + mu^2/(2\hbar^2)]^2 + \Delta^2}$. As the strength of the impurity potential $|u|$ increases, the bound state will move deeper below the Fermi sea.

To confirm that these results still hold when a trapping potential is present, as is always the case in the experiment, we add a harmonic potential $V_T = m\omega_0^2 x^2 / 2$ to the system and perform the calculation using the Bogoliubov-de Gennes (BdG) method [9–11]. The BdG equation can be written as

$$\begin{bmatrix} H_\uparrow^s - \mu_\uparrow & -\Delta \\ -\Delta^* & -H_\downarrow^s + \mu_\downarrow \end{bmatrix} \begin{bmatrix} u_\eta \\ v_\eta \end{bmatrix} = E_\eta \begin{bmatrix} u_\eta \\ v_\eta \end{bmatrix}, \quad (6)$$

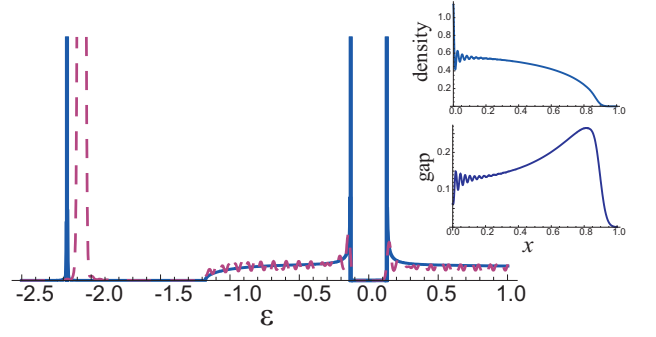


FIG. 1: (Color online) Local density of state (arb. units) at the site of a localized non-magnetic impurity with $u = -0.02E_F x_{TF}$, where E_F is the Fermi energy and $x_{TF} = \sqrt{N}a_{ho}$ ($a_{ho} = \sqrt{\hbar/(m\omega_0)}$) is the Thomas-Fermi radius of the non-interacting system. The dimensionless interaction parameter $\gamma = -mg/(\hbar^2 n_0) = 1.25$ where $n_0 = 2\sqrt{N}/(\pi a_{ho})$ is the peak Thomas-Fermi density of the non-interacting system. $N = 100$ is the total number of particles. The two spin components have equal population. Solid and dashed lines represent results obtained using the T -matrix and BdG method, respectively. The insets show the density and gap profile of the trapped system from the BdG calculation. The units for density, energy and length are n_0 , E_F and x_{TF} , respectively.

where $H_\sigma^s = -(\hbar^2/2m)d^2/dx^2 + V_T + U_\sigma + gn_\sigma$, $n_\uparrow = \sum_\eta |u_\eta|^2 \Theta(-E_\eta)$, $n_\downarrow = \sum_\eta |v_\eta|^2 \Theta(E_\eta)$ and $\Delta = -g \sum_\eta u_\eta v_\eta^* \Theta(-E_\eta)$, with $\Theta(\cdot)$ being the unit step function. The BdG equation above are solved self-consistently using a hybrid method whose details can be found in Ref. [10]. Once the solutions are found, we can calculate the LDOS at any points in space as $\rho_\uparrow(\epsilon) = \sum_\eta |u_\eta|^2 \delta(\epsilon - E_\eta)$ and $\rho_\downarrow(\epsilon) = \sum_\eta |v_\eta|^2 \delta(\epsilon + E_\eta)$. In practice, the δ -function in the expression of the LDOS is replaced by a Gaussian with a small width of $0.02 E_F$.

The dashed line in Fig. 1 represents the LDOS at the non-magnetic impurity site ($x = 0$) calculated using the BdG method. The agreement with the T -matrix method is satisfactory. The remaining discrepancies (in particular the position of the bound state) can be understood as the T -matrix method neglects the trapping potential and is not fully self-consistent: the values of the chemical potentials, densities and pairing gap used in the T -matrix calculation are taken to be those from the BdG result in the absence of the impurity. The insets of Fig. 1 demonstrate the density and gap profiles of the trapped system. The Friedel oscillation with a spatial frequency close to $2k_F$, where k_F is the Fermi wave number, can be easily identified near the impurity.

Figure 2(a),(b) display the LDOS at the magnetic impurity site for the two spin species, respectively. Again, we use the T -matrix method to study a homogeneous system and the BdG method to investigate the trapped system. Here the impurity potential is attractive (repulsive) for spin-up (-down) component. As a result, the bound state below the Fermi sea only exists for spin-up

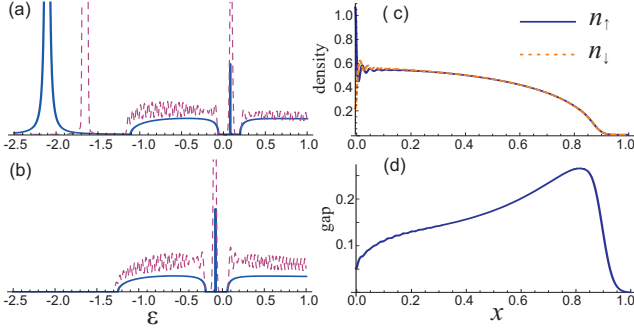


FIG. 2: (Color online) (a), (b) LDOS (arb. units) for spin up and down atoms at the site of a localized magnetic impurity. Solid and dashed lines represent results obtained using the T -matrix and BdG method, respectively. The density and gap profiles for the trapped system are presented in (c) and (d), respectively. Same parameters and units as in Fig. 1.

atoms. However, both $\rho_\uparrow(\epsilon)$ and $\rho_\downarrow(\epsilon)$ exhibit an additional resonance peak near $\epsilon = 0$, which signals the presence of a mid-gap bound state [12]. In addition, the magnetic impurity breaks the local spin balance, and results in a relative shift of the LDOS spectrum for the two spin components. The density and gap profiles are illustrated in Fig. 2(c),(d). Friedel oscillations can still be seen in the density profiles near the impurity. The magnetic impurity tends to break Cooper pairs, leading to a reduced gap size near the impurity as can be seen from Fig. 2(d). The quasiparticles originated from the broken pairs will populate the mid-gap bound state. In the weak interaction limit, the position of the mid-gap bound state can be found from the T -matrix method as

$$E_0 = \pm \Delta \frac{1 - (u\pi\rho_0/2)^2}{1 + (u\pi\rho_0/2)^2}, \quad (7)$$

where ρ_0 is the density of states at the Fermi sea, and the $+$ ($-$) sign refers to the spin-up (-down) component. The mid-gap bound state is thus located outside the band and inside the pairing gap. As the strength of the impurity $|u|$ increases, the mid-gap moves from the upper gap edge to the lower gap edge for spin-up component and moves oppositely for spin-down component.

Detection of the mid-gap state — As we have seen above, the mid-gap bound state induced by a magnetic impurity manifests itself in the LDOS. The LDOS provides valuable information of the quantum system. It is therefore highly desirable to construct a device that can measure the LDOS directly. In high T_c superconductors, the scanning tunneling microscope (STM), which measures the differential current that is proportional to the LDOS, is just such a device [13]. In ultracold atomic systems, radio-frequency (RF) spectroscopy [14–16] has become an important tool to probe the properties of Fermi gases. The RF field induces single-particle excitations by coupling one of the spin species (say $|\uparrow\rangle$ atoms) out of the pairing state to a third state $|3\rangle$ which is initially un-

occupied. In the experiment, the RF signal is defined as the average rate change of the population in state $|\uparrow\rangle$ (or state $|3\rangle$) during the RF pulse. The first generation RF spectrum gives the total current averaged over the whole atomic cloud, hence the interpretation of the RF signal is complicated by the trap inhomogeneity [17]. More recently the spatially resolved RF spectroscopy which provides the *local* information of the system has been demonstrated [18]. Here we show that a modified implementation of the spatially resolved RF spectroscopy can yield direct information of the LDOS.

To study the effect of the RF field, the total Hamiltonian now include two additional parts

$$H_3 = \int dx \psi_3^\dagger(x) \left[-\frac{\hbar^2}{2m} \frac{d^2}{dx^2} + V_3(x) - \nu - \mu_3 \right] \psi_3(x), \quad (8)$$

$$H_T = \int dx [T\psi_3^\dagger(x)\psi_\uparrow(x) + T\psi_\uparrow^\dagger(x)\psi_3(x)], \quad (9)$$

where H_3 represents the single-particle Hamiltonian of the state 3 (we assume that atoms in state 3 do not interact with other atoms), with V_3 being the trapping potential of the state and ν the detuning of the RF field from the atomic transition, H_T represents the coupling between state 3 and spin-up atoms. Since RF photon wavelength is much larger than typical size of the atomic cloud, the coupling strength T can be regarded as a spatially invariant constant. For weak RF coupling, one may use the linear response theory [19–21] to obtain the RF signal which is proportional to $I(x) = \frac{d}{dt} \langle \psi_3^\dagger(x)\psi_3(x) \rangle$. Under the linear response theory, we have

$$I(x) \propto \int dx' d\omega A_\uparrow(x, x'; \omega) A_3(x', x, \omega + \mu_\uparrow - \mu_3) f(\omega), \quad (10)$$

where $f(\omega)$ is the Fermi distribution function which reduces to the step function at zero temperature, A_α is the spectral function for state α . As state 3 is non-interacting, we have $A_3 = \sum_n \phi_n(x) \phi_n^*(x') \delta(\omega + \mu_\uparrow + \nu - \epsilon_n)$, where ϕ_n and ϵ_n are the single-particle eigenfunctions and eigenenergies of state 3, respectively. In the case where V_3 represents an optical lattice potential in the tight-binding limit, we may neglect the dispersion of state 3 as the lowest band is nearly flat. In other words, under such conditions, $\epsilon_n = \epsilon$ becomes an n -independent constant. Consequently $A_3(x, x') \sim \delta(x - x')$. At zero temperature, the RF signal then is directly related to the LDOS as

$$I(x) \propto \rho(x, -\mu_\uparrow - \nu + \epsilon) \Theta(\mu_\uparrow + \nu - \epsilon). \quad (11)$$

In this way, the spatially resolved RF spectroscopy becomes the analog of the STM.

Extended impurity — So far, we have focused on the effect of a localized impurity. Now we take the impurity potential to be a Gaussian with finite width $U_\sigma(x) = u_\sigma e^{-x^2/a^2}/(a\sqrt{\pi})$. When the width of the Gaussian impurity is small, the results we obtained are essentially the

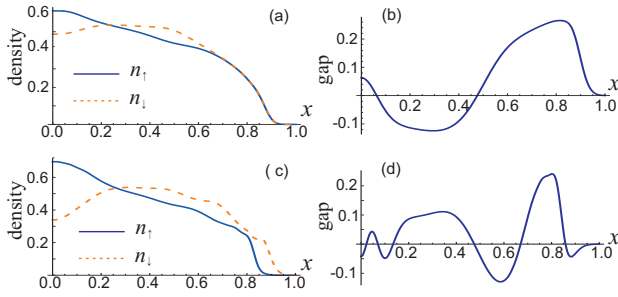


FIG. 3: (Color online) Density (a), (c) and gap (b), (d) profiles of a trapped system under an extended Gaussian magnetic impurity potential. The strength and the width of the impurity potential are (a) and (b): $u = u_{\uparrow} = -u_{\downarrow} = -0.16E_F x_{TF}$ and $a = 0.2x_{TF}$; (c) and (d): $u = u_{\uparrow} = -u_{\downarrow} = -0.4E_F x_{TF}$ and $a = 0.2x_{TF}$. Other parameters and units are the same as in Fig. 1.

same as the localized impurity. We will hence only show here the results of a magnetic impurity with relatively large width. Two examples of the density and gap profiles obtained from BdG equations are shown in Fig. 3. For an extended impurity potential with sufficient width, the Friedel oscillation is suppressed. By tailoring the strength and/or the width of the impurity, one can control the local spin imbalance. Under proper conditions, the gap profiles exhibit Fulde-Ferrell-Larkin-Ovchinnikov (FFLO)-like oscillations [22], which has become a very active research area in cold atoms recently [23–25]. The impurity therefore provides us with a controlled way to

create FFLO state.

In conclusion, we have investigated the effects of a single classical impurity in ultracold Fermi superfluid state. For a localized attractive non-magnetic impurity, there exists a bound state below the Fermi sea; for a localized magnetic impurity, a similar bound state occurs only in the spin component for which the impurity is attractive. However, the magnetic impurity will induce a mid-gap bound state inside the pairing gap for both spin species. We have proposed an STM-like scheme based on the spatially resolved RF spectroscopy to measure the local density of states, from which the mid-gap bound state can be unambiguously detected. Finally, we have considered an extended impurity potential. By manipulating the strength and the width of the impurity, one can realize the FFLO state in the system in a controlled manner.

In the future, it will also be interesting to study periodic or random arrays of localized impurities which may be exploited to induce novel quantum states in Fermi superfluids. Another interesting possibility is to consider a quantum impurity with its own internal degrees of freedom. Such a system may allow us to explore Kondo physics in cold atoms.

Acknowledgments

This work is supported by the NSF, the Welch Foundation (Grant No. C-1669) and by a grant from the Army Research Office with funding from the DARPA OLE Program. HH acknowledges the support from an ARC Discovery Project (Grant No. DP0984522).

-
- [1] A. V. Balatsky, I. Vekhter, and Jian-Xin Zhu, *Rev. Mod. Phys.* **78**, 373 (2006).
 - [2] H. Alloul *et al.*, *Rev. Mod. Phys.* **81**, 45 (2009).
 - [3] A.P. Mackenzie *et al.*, *Phys. Rev. Lett.* **80**, 161 (1998).
 - [4] P. T. Sprunger *et al.*, *Science* **275**, 1764 (1997).
 - [5] A. J. Millis, *Solid State Commun.* **126**, 3 (2003).
 - [6] G. Modugno, *Rep. Prog. Phys.* **73**, 102401 (2010).
 - [7] C. Zipkes *et al.*, *Nature* **464**, 388 (2010).
 - [8] P. J. Hirschfeld, D. Vollhard, and P. Wölfle, *Solid State Commun.* **59**, 111 (1986).
 - [9] P. de Gennes, *Superconductivity of Metals and Alloys* (Addison-Wesley, New York, 1966).
 - [10] X.-J. Liu, H. Hu, and P. D. Drummond, *Phys. Rev. A* **75**, 023614 (2007); X.-J. Liu, H. Hu, and P. D. Drummond, *Phys. Rev. A* **76**, 043605 (2007).
 - [11] L. O. Baksmaty *et al.*, arXiv:1003.4488.
 - [12] L. Yu, *Acta Phys. Sin.* **21**, 75 (1965); H. Shiba, *Prog. Theor. Phys.* **40**, 435 (1968); A. I. Rusinov, *Sov. Phys. JETP* **29**, 1101 (1969).
 - [13] Øystein Fischer *et al.*, *Rev. Mod. Phys.* **79**, 353 (2007).
 - [14] C.A. Regal and D.S. Jin, *Phys. Rev. Lett.* **90**, 230404 (2003).
 - [15] S. Gupta *et al.*, *Science* **300**, 1723 (2003).
 - [16] C. Chin *et al.*, *Science* **305**, 1128 (2004).
 - [17] P. Massignan, G. M. Bruun, and H. T. C. Stoof, *Phys. Rev. A* **77**, 031601(R) (2008).
 - [18] Y. Shin *et al.*, *Phys. Rev. Lett.* **99**, 090403 (2007).
 - [19] P. Törmä and P. Zoller, *Phys. Rev. Lett.* **85**, 487 (2000); G. M. Bruun *et al.*, *Phys. Rev. A* **64**, 033609 (2001).
 - [20] J. Kinnunen, M. Rodriguez, and P. Törmä, *Science* **305**, 1131 (2004); *Phys. Rev. Lett.* **92**, 230403 (2004).
 - [21] Y. He, Q. Chen, and K. Levin, *Phys. Rev. A* **72**, 011602(R) (2005); Y. He *et al.*, *Phys. Rev. A* **77**, 011602(R) (2008).
 - [22] P. Fulde and R. A. Ferrell, *Phys. Rev.* **135**, A550 (1964); A. I. Larkin and Y. N. Ovchinnikov *Sov. Phys.-JETP* **20**, 762 (1965).
 - [23] Y.-A. Liao *et al.*, *Nature* **467**, 567 (2010).
 - [24] G. Orso, *Phys. Rev. Lett.* **98**, 070402 (2007); H. Hu, X.-J. Liu, and P. D. Drummond, *Phys. Rev. Lett.* **98**, 070403 (2007).
 - [25] I. Zapata *et al.*, *Phys. Rev. Lett.* **105**, 095301 (2010); K. Sun *et al.*, arXiv:1009.4476v1.